LISTVENITE OCCURRENCES IN THE FAULT ZONES OF NORTHERN VICTORIA LAND, ANTARCTICA: ASTER-BASED MAPPING APPROACH

Amin Beiranvand Pour[1,2], Yongcheol Park[1], Jong Kuk Hong[1], Aidy M Muslim and Biswajeet Pradhan[3]

[1] Korea Polar Research Institute (KOPRI) Songdomirae-ro,Yeonsu-gu, Incheon 21990, Republic of Korea
[2]Institute of Oceanography and Environment (INOS), Universiti Malaysia Terengganu (UMT), 21030 Kuala Nerus, Terengganu, Malaysia
[3]School of Systems, Management and Leadership, Faculty of Engineering and Information Technology, University of Technology Sydney, New South Wales, Australia

Email: beiranvand.amin80@gmail.com; ypark@kopri.re.kr; jkhong@kopri.re.kr; aidy@umt.edu.my; Biswajeet.Pradhan@uts.edu.au

KEY WORDS: Listvenite; hydrothermal minerals; ASTER; Northern Victoria Land; Antarctica

ABSTRACT: Listvenite, a Mg-carbonate-quartz-fuchsite±Cr-chlorite±pyrite±chromite rock, forms by hydrothermal/metasomatic alteration of mafic and ultramafic rocks and represents a key indicator for hydrothermal mineral deposits in orogenic belts. Hydrothermal/metasomatic alteration zones in the damage zones of accretionary plate boundaries are efficiently detected using multispectral satellite remote sensing data. In this research, Advanced Spaceborne Thermal Emission and Reflection Radiometer (ASTER) multispectral remote sensing data are used to identify listvenite occurrences and alteration mineral zones in the poorly exposed damage zones of the boundaries between the Wilson, Bowers and Robertson Bay terranes in Northern Victoria Land (NVL) of Antarctica. Spectral information for detecting alteration mineral assemblages and listvenite zones were extracted at pixel and sub-pixel levels using the Principal Component Analysis (PCA)/Independent Component Analysis (ICA) fusion technique, Linear Spectral Unmixing (LSU) and Constrained Energy Minimization (CEM) algorithms. Mineral phases containing Fe2+, Fe3+, Fe-OH, Al-OH, Mg-OH and CO3 spectral absorption features were are distinguished in the damage zones through PCA/ICA fusion of ASTER visible and near infrared (VNIR) and shortwave infrared (SWIR) bands of ASTER. Silicate rocks are discriminated from the PCA/ICA fusion of the ASTER thermal infrared (TIR) bands. The extracted mineral images of goethite, hematite, jarosite, biotite, kaolinite, muscovite, antigorite, serpentine, talc, actinolite, chlorite, epidote, calcite, dolomite and siderite and listvenite occurrences were produced using the LSU and CEM algorithms. Listvenite occurrences are confined to mafic metavolcanic rocks (Glasgow Volcanics) in the Bowers Mountains. New field investigations verified the presence of listvenite in the mapped zones and further constrain on the efficiency of the integrative methodology used in this study.

1. INTRODUCTION

Listvenite is a metasomatic rock composed of variable amounts of quartz, magnesite, ankerite, dolomite, sericite, calcite, talc and sulfide minerals. It is formed by interaction of mafic and ultramafic rocks with low to intermediate temperature CO2- and S-rich fluids, and commonly found along the major fault and shear zones at terrane boundaries or major tectonic units in orogenic systems. As such, listvenite is spatially associated with ophiolites, greenstone belts and suture zones in orogenic belts (Zoheir and Lehmann, 2011). Advanced Spaceborne Thermal Emission and Reflection Radiometer (ASTER) multispectral remote sensing satellite data provide appropriate spatial, spectral and radiometric resolutions suitable for mapping hydrothermal/metasomatic alteration mineral assemblages (Pour et al., 2019a,b, 2018a,b,c,d; Noori et al., 2019; Sheikhrahimi, 2019).

Iron oxide/hydroxide, hydroxyl-bearing and carbonate mineral groups present diagnostic spectral absorption features due to electronic processes of transition elements (Fe2+, Fe3+ and REE) and vibrational processes of fundamental absorptions of Al-OH, Mg-OH, Fe-OH, Si-OH, CO3, NH4 and SO4 groups in the visible and near infrared (VNIR) and shortwave infrared (SWIR) regions (Cloutis et al., 2006). These mineral groups can be detected using three VNIR (from 0.52 to 0.86 μm; 15-m spatial resolution) and six SWIR (from 1.6 to 2.43 μm; 30-m spatial resolution) spectral bands of ASTER (Abrams et al., 2004). Additionally, thermal infrared bands (TIR; 8.0–14.0 μm; 90-m spatial resolution) of ASTER are capable of discriminating silicate lithological groups due to different characteristics

of the emissivity spectra derived from Si–O–Si stretching vibrations in the TIR region (Ninomiya and Fu, 2018). In Northern Victoria Land (NVL) of Antarctica, the widespread occurrence of listvenites was documented as one of the main types of hydrothermal/metasomatic fault-related rocks in the damage zones between the Wilson Terrane (WT) and the Bowers Terrane (BT) (Fig. 1) (Crispini and Capponi, 2002). Recently, remote sensing studies have been conducted by Pour et al. (2018 a,b) for regional- scale lithological mapping in NVL and local-scale alteration mineral mapping in the Morozumi Range and Helliwell Hills areas of the WT. However, no comprehensive remote sensing study is available so far for the boundary region between the WT and the BT further to the east, where particularly listvenite bodies occur in the damage zones.
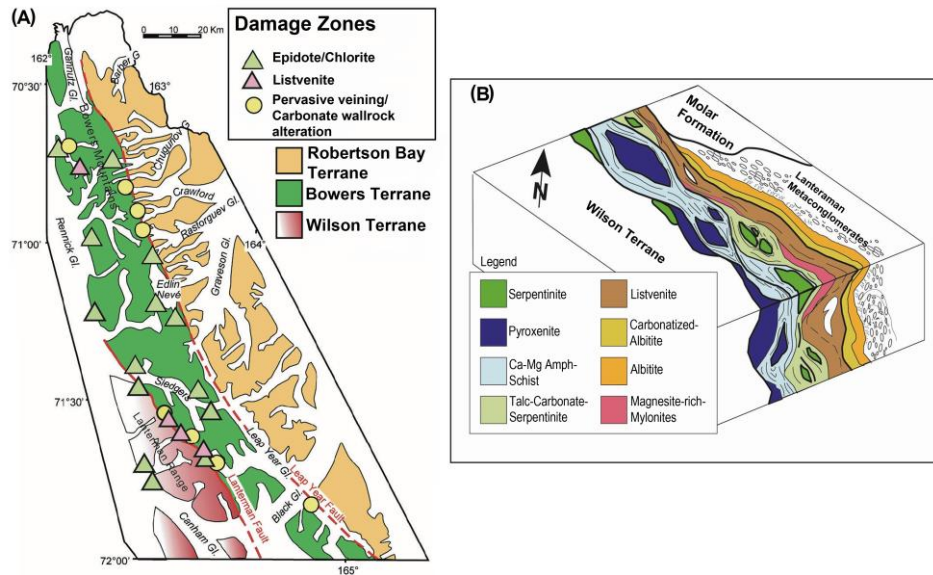

Figure 1. (A) Sketch map with the location of the damage zones where the hydrothermal alteration and veining is more intense. (B) Sketch map of lithological-mineralogical sequences in the damage zone at the boundary of WT and BT (Modified from Crispini and Capponi, 2002).

2.   MATERIALS AND METHODS

2.1   Remote sensing data

Twelve ASTER level 1T (Precision Terrain Corrected Registered At-Sensor Radiance) scenes obtained from U.S. Geological EROS (http://glovis.usgs.gov/) were used for mapping the poorly exposed damage zones of the WT-BT boundary. Atmospheric correction was applied to the ASTER data using Fast Line-of-sight Atmospheric Analysis of Spectral Hypercube (FLAASH) algorithm. The ASTER images were pre-georeferenced to UTM zone 58 South projection using the WGS-84 datum and rotated to north up UTM projection. Furthermore, the 30-meter resolution SWIR bands were re-sampled to 15-meter spatial dimensions (correspond to the VNIR 15-m resolution) using the nearest neighbour re-sampling technique for producing a stacked layer of VNIR+SWIR bands.

2.2   Data analysis

Spectral information to detect alteration mineral assemblages and listvenites in the damage zones of the WT-BT boundary were extracted at the pixel and sub-pixel levels using specialized/standardized image processing algorithms. For regional scale mapping of the WT-BT boundary, pixel-based algorithms, including Principal Component Analysis (PCA) and Independent Component Analysis (ICA) were used. Sub-pixel-based algorithms, namely Linear Spectral Unmixing (LSU) and Constrained Energy Minimization (CEM) were applied for detailed mapping in some selected subsets of the damage zones at the local scale. Flowchart of the methodology used in this research is shown in Figure 4. For processing the datasets, the ENVI (Environment for Visualizing Images, http://www.exelisvis.com) version 5.2 and ArcGIS version 10.3 (Esri, Redlands, CA, USA) software packages were used.
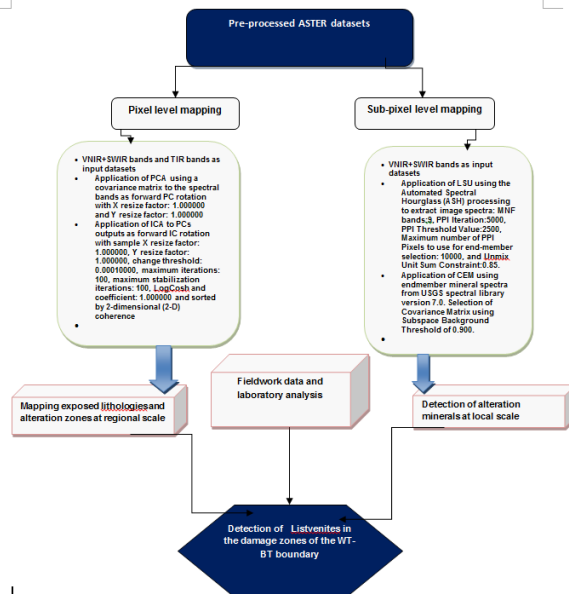
Figure 2. An overview of the methodological flowchart used in this study.

3. RESULTS AND DISCUSSION

The PCA5, PCA7 and PCA6 were assigned to RGB color composite for mapping iron oxide/hydroxide minerals, Al-OH minerals and Fe,Mg-O-H and CO3 minerals, respectively. Figure 3 (A) shows the resultant image-map for the spatial subset covering zone 1 and the surrounding areas. Magenta, red, yellow and light yellow pixels are dominated in the exposed zones and green and blue pixels are less in abundance (Fig. 3 A). Thus, iron oxide/hydroxide minerals have high surface abundance in the exposed lithologies in zone 1. However, Al-OH minerals and Fe,Mg-O-H and CO3 mineral assemblages have low surface abundance and are generally associated with iron mineral groups as magenta, yellow and light yellow pixels. With reference to the geological map of the zone 1 and surrounding areas, the exposed lithological units mostly consist of Wilson Terrane metamorphic rocks, Granite Harbour Igneous Complex, Beacon Supergroup and Ferrar Dolerite. Surface distribution of iron oxide/hydroxide minerals (red and magenta pixels) is typically associated with the Ferrar Dolerite and Granite Harbour Igneous Complex (Fig. 3 A), for instance the exposures of Ferrar Dolerite in the northern part of the Alamein Range and the exposed zones of the Granite Harbour Igneous Complex along the Hunter Glacier in the southern part of the Lanterman Range. The Al-OH and Fe,Mg-O-H and CO3 minerals (green, blue, yellow and light yellow pixels) are mainly concentrated in exposures of the Beacon Supergroup and Wilson Terrane metamorphic rocks (particularly amphibolite-facies metasedimentary rocks).

The PCA3, PCA7 and PCA6 were selected for ICA rotation and subsequent RGB color composite to detect iron oxide/hydroxide, Al-OH and Fe,Mg-O-H and CO3 minerals, respectively. Figure 3 (B) displays the resultant image-map for the spatial subset covering zones 2 and 3. Several types of mineral assemblages are detected. Prevalent distribution of iron oxide/hydroxide minerals (red and magenta pixels) is associated with most of the exposures, while Al-OH minerals (green pixels) and Fe,Mg-O-H and CO3 minerals (blue pixels) are specifically dominated in some exposed zones. The admixture of the mineral groups (yellow and cyan pixels) is also observable in some small exposures (Fig 3 B). Comparison with the geological map of the study zones indicates that iron oxide/hydroxide minerals are typically associated with exposures of the Granite Harbour Igneous Complex of the WT, Glasgow metavolcanic rocks of the BT, Robertson Bay Group of the RBT and Admiralty Intrusives. The Al-OH minerals and Fe,Mg-O-H and CO3 minerals characterize the exposed zones of metasedimentary rocks (the Molar Formation, Mariner Group and Leap Year Group) of the BT, Wilson Terrane metamorphic rocks and Ferrar Dolerite.

Figure 3 (C) displays the resultant image-map for the spatial subset covering zone 4 and the surrounding areas. The iron oxide/hydroxide mineral group appears as red and magenta color pixels, which are mainly dominated in exposed lithologies associated with the Litell Rocks region (consists of Kirkpatrick Basalts/Ferrar Dolerite) in the south-western part of the image. The Al-OH mineral group represents as green and cyan color pixels, which are associated with exposed rocks in the Bowers Mountains (Fig. 3 C). Conceivably, they are exposures of the Molar Formation and the Mariner Group that contain a high content of clay minerals. The Fe,Mg-O-H and CO3 minerals manifest in blue color pixels, which have low surface abundance in the study zone. However, they are generally

associated with iron oxide/hydroxide minerals in several exposed zones (Fig. 3 C). Possibly, the exposures contain a high content of Fe,Mg-O-H and iron oxide/hydroxide minerals in the Bowers Mountains are Glasgow metavolcanic rocks of the BT. The Autobahn Moraine is a prominent and linear large moraine stretching over several 10s of kilometres along the Rennick Glacier (GANOVEX Team, 1987). The iron oxide/hydroxide and Al-OH mineral groups are mapped in the Autobahn Moraine (the central part of Fig. 3 C).
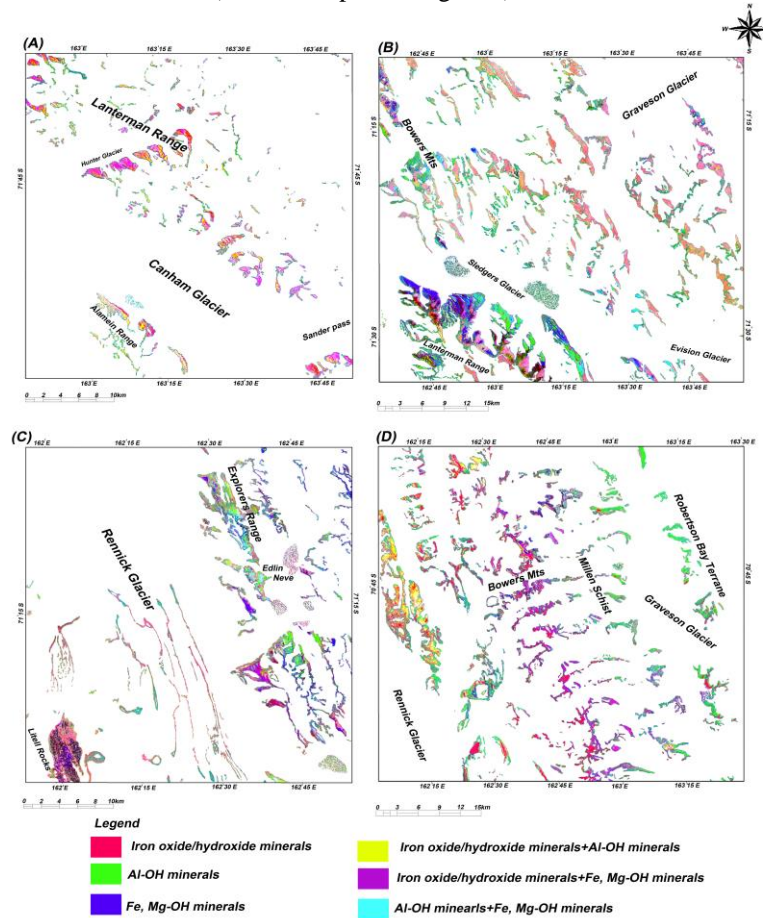

Figure 3. ASTER image-maps derived from the ICA rotation and subsequent RGB color composite to VNIR+SWIR bands. (A) Spatial subset covering zone 1 and surrounding areas; (B) Spatial subset covering zones 2 and 3; (C) Spatial subset covering zone 4 and surrounding areas; and (D) Spatial subset covering zones 5 and 6.

Figure 3 (D) shows the resultant image-map for the spatial subset covering zones 5 and 6, which covers the Bowers Mountains, Millen Schist and Robertson Bay Terrane (RBT) from west to east. Magenta, red, yellow and green pixels are governed in most of the exposures, while blue pixels are very less in abundance. Hence, iron oxide/hydroxide and Al-OH mineral groups and their admixture are dominant mineral assemblages in the study zone. The Glasgow Volcanics, the Molar Formation, Millen Schist, Robertson Bay Group and Admiralty Intrusives are exposed in the zones 5 and 6 with reference to the geological map. It is discernible that the exposures of Glasgow Volcanics and Admiralty Intrusives contain a high surface distribution of iron oxide/hydroxide with some admixture of Al-OH minerals, which appear as magenta, red and yellow pixels in Figure 3 (D). The Molar Formation, Millen Schist and Robertson Bay Group appear in green color pixels due to the high content of Al-OH mineral assemblages (Fig. 3 D). Figure 4 (A) shows the LSU classification mineral map for the zone (1). Results indicate that the goethite/hematite/jarosite group is spectrally governed the zone (1), while biotite/muscovite and kaolinite groups have less contribution in total mixed spectral characteristics. In zone (1), the Wilson Terrane metamorphic rocks, Granite Harbour Igneous Complex, Beacon Supergroup and Ferrar Dolerite are exposed. Therefore, a high surface abundance of iron oxide/hydroxide minerals is related to crystal-field transitions of iron ions (Fe+2 and Fe+3) in the primary mafic minerals (olivine, pyroxenes and plagioclase) and/or the alteration of primary mafic minerals within mafic rock units such as the Wilson Terrane metamorphic rocks and Ferrar Dolerite. Kaolinite high abundance zones are mostly associated with the detrital clay minerals of the Beacon Supergroup. Biotite/muscovite group seems to be phyllic alteration zone associated with the Granite Harbour Igneous Complex. Accordingly, the presence of listvenite bodies in the zone (1) is slightly feasible.

Figure 4 (B) shows the resultant classification map for the subset of the zone (2). Goethite/hematite/jarosite and chlorite/epidote/actinolite groups show high surface abundance, whereas kaolinite and biotite/muscovite groups exhibit moderate to less spectral contribution and spatial distribution in zone (2). The association of

goethite/hematite/jarosite and chlorite/epidote/actinolite groups is observable with exposures of the Glasgow metavolcanic rocks and metasedimentary rocks (Molar Formation, Mariner Group and Leap Year Group). Kaolinite, biotite/muscovite and iron oxide/hydroxide assemblages are associated with the Granite Harbour Igneous Complex. The Wilson Terrane metamorphic rocks and Ferrar Dolerite exposures are generally dominated by goethite/hematite/jarosite group, while the Beacon Supergroup is governed by kaolinite group. For that reason, listvenite bodies could be located in a zone that spatially contains all of the four alteration mineral assemblages. Note that the large greenish-colored spot in the area of the Sledgers Glacier is a dense crevasse field, which may contain contamination of clay mineral groups (Fig. 4 B). Several prospect zones for listvenite bodies are identifiable in zone (2); some of them are delimited by yellow rectangles in Figure 4 (B).
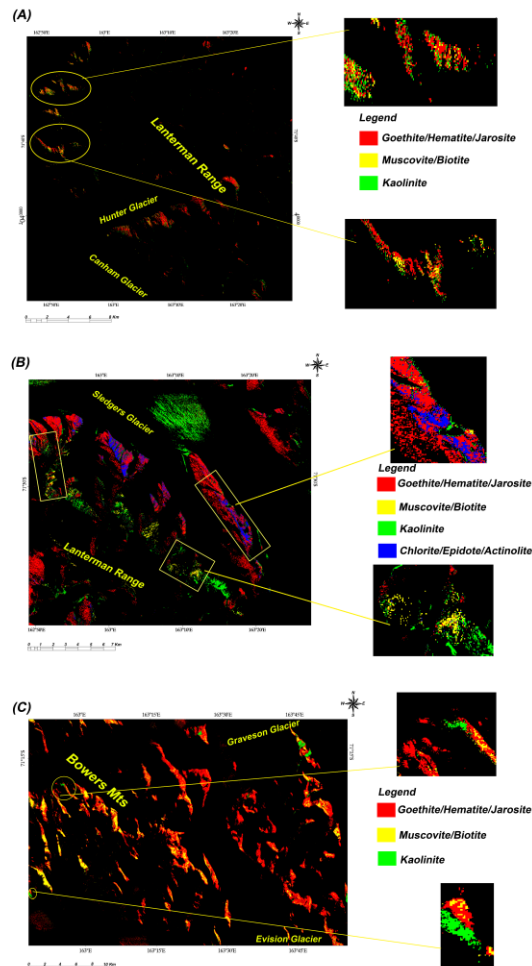

Figure 4. LSU classification mineral maps derived from fraction images of the extracted end-members. (A) Zone 1; (B) Zone 2; (C) Zone 3. Spectrally dominant mineral groups (concertation more than 10%) depict as colored pixels.

Figure 4 (C) displays LSU classification mineral map for the zone (3). Goethite/hematite/jarosite and biotite/muscovite groups are spectrally dominated. Kaolinite group shows very low surface abundance. Iron oxide/hydroxide and biotite/muscovite mineral groups are concentrated in the exposures of the Glasgow metavolcanic rocks and metasedimentary rocks in the Bowers Mountains. Small exposures of the Granite Harbour Igneous Complex and Admiralty Intrusives contain kaolinite group minerals associated with iron oxide/hydroxide and biotite/muscovite mineral groups, which can be attributed to the alteration products of argillic and phyllic alteration zones. Hence, the zone (3) has very low potential for containing listvenites.

The CEM algorithm was implemented to produce fraction images of selected end-member spectra from the USGS spectral library, including goethite, hematite, jarosite, biotite, kaolinite, muscovite, antigorite, serpentine, talc, actinolite, chlorite, epidote, calcite, dolomite, siderite and chalcedony. Therefore, some of the target alteration minerals may have a similar manifestation of the fractional abundances in the CEM rule images. For iron oxide/hydroxide mineral group, fractional abundances of goethite and hematite show almost similar appearance and high mixtures, while jarosite shows low mixtures with them and different spatial fractional abundance in some parts of the zone (2).

4. CONCLUSIONS

Application of ASTER multispectral remote sensing data for detecting hydrothermal alteration mineral assemblages and particularly listvenites in the poorly exposed damage zones of the WT-BT boundary, the BT-RBT boundary and within the BT and in the eastern WT (NVL, Antarctica) confirmed the alteration mineral patterns at several locations, including the predominance of iron oxide/hydroxide, biotite/muscovite, chlorite/epidote/actinolite, Mg-Ca-Fe carbonates and listvenites. The mapping results indicate that ASTER data processing using the pixel/sub-pixel algorithms can provide an efficient approach to map hydrothermal alteration minerals, lithological units (ultramafic, mafic, intermediate and felsic) and listvenite occurrences in inaccessible parts of the NVL and can be broadly applicable in other tectonic boundaries or major tectonic damage zones around the world.

REFERENCES

Abrams, M., Hook, S. and Ramachandran, B., 2004. ASTER User Handbook, Version 2. Jet Propulsion Laboratory, California Institute of Technology. Online: http://asterweb.jpl. nasa.gov/content/03_data/04_Documents/aster_ guide_ v2.pdf. (accessed on 21 September 2015).

Cloutis, E.A., Hawthorne, F.C., Mertzman, S.A., Krenn, K., Craig, M.A., Marcino, D., et al., 2006. Detection and discrimination of sulfate minerals using reflectance spectroscopy. Icarus 184, 121–157.

Ninomiya, Y., Fu, B., 2018. Thermal infrared multispectral remote sensing of lithology and mineralogy based on spectral properties of materials. Ore Geology Reviews, doi:10.1016/j.oregeorev.2018.03.012

Noori, L., Pour, B.A., Askari, G., Taghipour, N., Pradhan, B., Lee, C-W., Honarmand, M., 2019. Comparison of Different Algorithms to Map Hydrothermal Alteration Zones Using ASTER Remote Sensing Data for Polymetallic Vein-Type Ore Exploration: Toroud–Chahshirin Magmatic Belt (TCMB), North Iran. Remote Sensing, 11 (5), 495; doi.org/10.3390/rs11050495.

Pour, A.B., Hashim, M., Hong, J.K., Park, Y. 2019a. Lithological and alteration mineral mapping in poorly exposed lithologies using Landsat-8 and ASTER satellite data: north-eastern Graham Land, Antarctic Peninsula. Ore Geology Reviews, 108, 112-133.

Pour, A.B., Park, Y., Crispini, L., Läufer, A., Kuk Hong, J., Park, T.-Y.S., Zoheir, B., Pradhan, B., Muslim, A.M., Hossain, M.S., Rahmani, O. 2019b. Mapping Listvenite Occurrences in the Damage Zones of Northern Victoria Land, Antarctica Using ASTER Satellite Remote Sensing Data. Remote Sensing 11, 1408. doi.org/10.3390/rs11121408.

Pour, A.B., Park, Y., Park, T.S., Hong, J.K. Hashim, M., Woo, J., Ayoobi, I., 2018a. Evaluation of ICA and CEM algorithms with Landsat-8/ASTER data for geological mapping in inaccessible regions. Geocarto International, doi.org/10.1080/10106049.2018.1434684

Pour, A.B., Park, Y., Park, T.S., Hong, J.K. Hashim, M., Woo, J., Ayoobi, I., 2018b. Regional geology mapping using satellite-based remote sensing approach in Northern Victoria Land, Antarctica. Polar Science 16, 23-46.

Pour, A.B., Park, T.S., Park, Y., Hong, J.K. Zoheir, B., Pradhan, B., Ayoobi, I. Hashim, M., 2018c. Application of multi-sensor satellite data for exploration of Zn-Pb sulfide mineralization in the Franklinian Basin, North Greenland. Remote Sensing 10, 1186; doi:10.3390/rs10081186.

Pour, A.B., Hashim, M., Park, Y., Hong, J.K., 2018d. Mapping alteration mineral zones and lithological units in Antarctic regions using spectral bands of ASTER remote sensing data. Geocarto International 33 (12), 1281-1306.

Sheikhrahimi, A., Pour, B.A., Pradhan, B., Zoheir, B., 2019. Mapping hydrothermal alteration zones and lineaments associated with orogenic gold mineralization using ASTER remote sensing data: a case study from the Sanandaj-Sirjan Zone, Iran. Advances in Space Research 63, 3315-3332.

Zoheir, B., Lehmann, B., 2011. Listvenite-lode association at the Barramiya gold mine, Eastern Desert, Egypt. Ore Geol. Rev. 39, 101–115.